EUROGRAPHICS - IEEE VGTC Symposium on Visualization (2005)
K. W. Brodlie, D. J. Duke, K. I. Joy (Editors)

VIS-a-VE: Visual Augmentation for Virtual Environments in Surgical Training

Adrian J. Chung,[1] Fani Deligianni,[1] Pallav Shah,[2] Athol Wells[2] and Guang-Zhong Yang[1]

[1] Royal Society/Wolfson Foundation Medical Image Computing Laboratory, Imperial College, London, UK
[2] Royal Brompton and Harefield NHS Trust

Abstract

Photo-realistic rendering combined with vision techniques is an important trend in developing next generation surgical simulation devices. Training with simulator is generally low in cost and more efficient than traditional methods that involve supervised learning on actual patients. Incorporating genuine patient data in the simulation can significantly improve the efficacy of training and skills assessment. In this paper, a photo-realistic simulation architecture is described that utilises patient-specific models for training in minimally invasive surgery. The datasets are constructed by combining computer tomographic images with bronchoscopy video of the same patient so that the three dimensional structures and visual appearance are accurately matched. Using simulators enriched by a library of datasets with sufficient patient variability, trainees can experience a wide range of realistic scenarios, including rare pathologies, with correct visual information. In this paper, the matching of CT and video data is accomplished by using a newly developed 2D/3D registration method that exploits a shape from shading similarity measure. Additionally, a method has been devised to allow shading parameter estimation by modelling the bidirectional reflectance distribution function (BRDF) of the visible surfaces. The derived BRDF is then used to predict the expected shading intensity such that a texture map independent of lighting conditions can be extracted. Thus new views can be generated that were not captured in the original bronchoscopy video, thus allowing free navigation of the acquired 3D model with enhanced photo-realism.

Categories and Subject Descriptors (according to ACM CCS): I.3.7 [Three-Dimensional Graphics and Realism]: I.4.8 [Scene Analysis]: J.3 [Medical Training]:

1. Introduction

Over the past decade there have been major advances in minimal access surgery, especially in the endoscopy field, which encompases bronchoscopy and laparoscopy. Endoscopy is the most common procedure in minimal access surgery and is carried out through natural body openings or small incisions made during surgery. With this technique, improvements in diagnostic accuracy and therapeutic success are significant when compared to conventional techniques, while at the same time patient trauma and hospitalisation time are greatly reduced. However, due to the complexity of instrument control particularly in the presence of mis-alignment of motion and visual axes, restrictions on vision and mobility, difficulties in hand-eye co-ordination, and limited tactile perception, a high degree of manual dexterity is required of the operator. To address this problem, new training methods are being actively researched for efficient acquisition and assessment of minimally invasive surgical (MIS) skills. The advantages of computer simulated endoscopic training over traditionally performed one-to-one apprenticeship schemes are now well accepted in the medical community. In this paper the current state of the art in patient specific modelling is discussed in light of recent research results [CDS*04, DCY03] applied to the field of bronchoscopy.

For certain MIS procedures, such as colonoscopy and bronchoscopy, effective simulators can be implemented using simple hardware [HSH*99], but for others such as laparoscopic cholesysectomy, difficult research issues persist. The deformation of human organs is not trivial to model, especially when the manipulation by medical instruments is considered. Furthermore, in most practical computer simulations, visual realism is severely lacking. Thus far, proto-

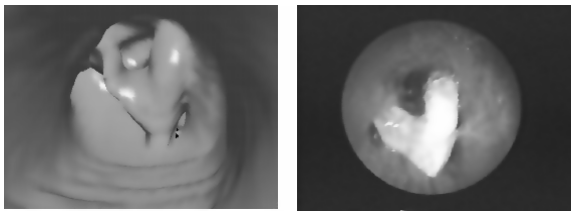

Figure 1:

type systems for minimal access surgical simulators have been developed for training in colonoscopy [GHW92], laparoscopy [MG97], bronchoscopy [CYC*97] and other surgical techniques. A number of factors, such as support for realistic tactile feedback, have limited the success of these systems. Most endoscope simulation systems have used standard polygon rendering techniques with synthetic texture mapping. Although visually the results can be quite impressive, the structure and appearance bares little resemblance to video acquired in vivo. Uniform texture mapping has often been applied throughout the model, and when rendering special visual effects, such as polyps or inflammation, both accuracy and adaptability are severely lacking [HJR*96]. The generation of realistic structure and surface properties has hindered the production of generic test case databases, since parts of the anatomy, such as the colon or the bronchi, exhibit considerable diversity in shape and texture. Figure 1 illustrates the shortcomings of virtual worlds modelled using only polygon rendering and uniform texture mapping. The left image was created by polygon rendering of CT scan data of the bronchi. The right image shows the same part of the bronchi as seen by a bronchoscope, revealing the unusual structure to be part of a broken dental prosthesis. In the absence of real video data that has been matched to the 3D structure, an accurate image cannot be constructed in simulation.

Due to the size and diversity of the data involved, the characterisation and representation of visual information remains a major challenge in visual realism. Early studies of virtual bronchoscopy have been a motivating factor in visual augmentation of virtual bronchoscopy through the incorporation of endoscopic video. The feasibility of such an idea has been investigated by a number of research groups for tracking camera motion and navigation planning [KYJ*02]. The architecture proposed in this paper will address the challenges of creating genuine surface texture information by making use of normally acquired video and tomographic data. Video data from real endoscopic procedures is obtained and matched to the geometry derived from CT images and the resulting hybrid dataset is explored by trainees through interaction with the simulation. This offers a visually accurate training environment, and opens up the possibility of training on a wide variety of real patient data, illustrating both natural diversity and particular pathognomonic cases.

The overall steps involved in the Vis-a-Ve framework include:

- Segmentation of 3D CT scan of the chest for extracting the bronchial tree which is reconstructed as a polygonal mesh
- Pre-processing the bronchoscopy video to remove interlacing and geometrical distortion
- 2D/3D registration of bronchoscopy video with CT scan
- Estimation of illumination parameters by modelling the intrinsic surface reflectance properties by backprojecting the video image on to the 3D mesh
- Extraction of illumination independent texture map
- Creation of a global texture map which, together with the surface illumination characteristics and the 3D polygonal model for generating realistic new views of the bronchial lumen.

1.1. 2D/3D Registration

Matching of video bronchoscope images to three-dimensional reconstructions of the bronchi requires robust 2D/3D registration. This technique involves optimising a similarity measure, which evaluates how close the model viewed from a given camera pose is to the current 2D video frame. Existing 2D/3D registration algorithms typically employ intensity [SHH98] and feature based techniques [CR03]. Intensity based techniques compare a projected image of the object with the 2D image, without any structural analysis based on similarity measures such as cross-correlation [MDS*02] and mutual information [Vio97]. Mutual information exploits the statistical dependency of two datasets and is particularly suitable for multi-modal images. These existing methods tend to make special illumination assumptions which are not applicable in bronchoscopy. In bronchoscope images, the light source is close to the tissue surface and inter-reflections become significant. Furthermore, the use of point light sources implies that power decreases with the square of the distance so it is essential to match the illumination conditions of the rendered 3D model in order for the intensity-based techniques to work. The method, however, is further complicated by specular reflections due to mucus coatings, and this can be difficult to model in practice.

1.2. Image Based Modelling and Rendering

One of the major challenges of combining 2D video with 3D morphological data for patient specific simulation is the extraction of intrinsic surface texture and reflectance properties that are not dependent on specific viewing and illumination conditions. This allows the generation of new views with different camera and lighting configurations. For surgical simulation, this permits the incorporation of tissue instrument interaction, and thus greatly enhances the overall realism of the simulation environment.

Highly realistic images can be obtained using global illumination methods, however the success of these techniques depends on the accurate modelling of the bidirectional reflectance distribution function, $\rho(\theta_i, \phi_i, \theta_r, \phi_r)$, where (θ_i, ϕ_i) and (θ_r, ϕ_r) are respectively the incoming and outgoing directions given in polar coordinates. A variety of functions have been proposed for ρ that cater for specific classes of materials [HTSG91]. Some BRDF models have a large number of parameters to adjust in order to match the characteristics of the target material, and there is often no robust way to ensure accuracy of the values chosen. Simpler models have been proposed that allow optimisation techniques to be used for parameter estimation [LW94] but these methods rely on measurements of surface reflectance over a wide range of illumination directions and intensities. In general, a great degree of control over lighting conditions is required to ensure adequate coverage of the high-dimensional domain over which ρ is defined. For this purpose, special reflectance measurement apparatus must be used [DvGNK99]. The strategy of measuring point reflectances can be extended to entire images, allowing one can measure an entire set of BRDFs and map them as a texture map over the surface of an object of known geometry [LKG*03].

If one has limited control over the lighting environment, an approach based on inverse global illumination may be pursued. A finite number of images captured from predetermined view points are used to determine the outgoing light intensities for several points in the environment. This enables their BRDFs to be determined by inverting the Rendering Equation [YDMH99]. To achieve this, it requires a large number of images to be captured from a wide range of directions and viewpoints. However, by making assumptions on the uniformity of the materials in the scene, the number of input images can be reduced significantly [BG01]. With bronchoscopy video, one has very limited control over the lighting conditions and the tubular structure of the airways restricts the choice of viewpoints and viewing angle. For this reason, a certain degree of uniformity of the reflectance in the bronchial lumen is assumed in the design of the bronchoscopy simulation framework.

2. In vivo patient study

For this study, bronchoscopy examination was performed on each patient according to a conventional clinical protocol. During the bronchoscopy procedure a prototype videoscope (Olympus BF Type; with field of view 120°) was used. Video images from the bronchoscopic examination were transferred to digital videotapes in PAL format at 25fps. Since the original endoscopic video frames contain both the endoscopic image and redundant black background, only the endoscopic view was digitised and cropped to images of 454×487 pixels. All images were converted to greyscale prior to registration. The CT images were acquired from the Siemens Somaton Volume Zoom four-channel multi-detector CT scanner with a slice width of 3mm and collimation of 1mm, and the acquisition volume covered from the aortic arch to the dome of the hemi-diaphragm. The bronchial tree was segmented from the other parts of the anatomy using region growing and morphological operators. Subsequently, the airway surface was reconstructed as a polygonal mesh by using the marching cubes algorithm. This mesh was then registered with the image frames captured from the video output of the bronchoscope with the aim of pairing each video frame with a corresponding camera pose within the airway.

3. Image Based Modelling and Rendering

An integral part of the proposed training simulation architecture is a novel technique for the recovery of intrinsic visual properties of the surface using BRDF modelling. An essential part of this process is the factoring of each video image into a surface shading function and texture map, as this enables new viewpoints to be visualised. With the effective use of 2D/3D registration, intrinsic surface reflectance properties can be recovered and used to generate new images during free navigation of the 3D model that are morphologically accurate and visually photo-realistic.

3.1. 2D/3D Registration

The 2D/3D registration procedure, described in detail in Fani et al [DCY03] consists of extracting surface normals from the video frames using a linear shape from shading technique and matching them with the surface normals specified from the 3D model. By processing 3D information instead of correlating intensity values increases robustness, improves immunity to variations in illumination conditions, and does not require expensive feature extraction. Finally, local deformations can be identified and tracked through out the endoscopy video and the similarity measure can be adjusted to compensate for it. The process of the proposed technique comprises the following major steps:

- Surface normal estimation for each pixel of the video image using a linear local shape-from-shading algorithm derived from the unique camera/lighting constraints of the endoscope.
- Extraction of the pq components of the 3D tomographic model by direct z-buffer differentiation.
- Applying a similarity measure based on angular deviations of the pq vectors derived from 2D and 3D data sets.

3.1.1. Shape from Shading

For video image sequences of the bronchoscopy, the geometrical information of the airways must be derived from the shading information. The problem of determining surface gradients from a grey shaded image has been an active area of research dating back to Horn's work [Hor77]. Direct application of the method, however, has encountered major

difficulties due to the non-parallel light source and perspective projection in endoscope, which results in a non-linear system of equations that suffers convergence difficulties. In addition, the albedo is not a constant and the surface is not purely Lambertian but has some specularity and at some places specular highlights.

In the specific case of using perspective projection with a point light source near the camera, the use of intensity gradient can reduce the conventional shape-from-shading equations to a linear form, which suggests a local shape-from-shading algorithm that avoids the complication of changing surface albedos. Unfortunately, bronchoscopy is a special case because the light source is very close to the camera and relatively close to the lumen surface, so conventional algorithms are not applicable. Recently, Prados [PF04] has studied the Lambertian shape-from-shading problem for pinhole camera with a point light source located at the optical centre. However, the intensity of the image is also affected from the distance between the surface point and the light source. Rashid [RB92] modelled this dependency by introducing a monotonically decreasing function, $f(r)$, so that the image irradiance, E, can be formulated as:

$$E(x,y) = s_0 \rho(x,y) \cos(i) f(r) \tag{1}$$

where s_0 is a constant related to the camera, ρ is the surface albedo and i is the angle between the incident light ray and the surface normal, $\vec{n} = [p,q,-1]$. Adopting the linear technique of Rashid [RB92] enabled the gradient vectors pq to be estimated by using a linear local shape-from-shading algorithm.

3.1.2. pq-space from 3D Reconstruction

It is relatively straightforward to extract the pq-components from the 3D model that was reconstructed from the CT data. Differentiation of the z-buffer for the rendered 3D surface, making use of $p = \partial z/\partial x$ and $q = \partial z/\partial y$, yields the required pq distribution and also elegantly avoids the tasks of occlusion handling. The effect of perspective projection has been taken into account during the rendering stage. The viewing frustum was tuned to cater for the fact that modern video-based endoscopes have a wide-angle field of view to allow greater detail at the centre of the display.

3.1.3. Similarity Measure

Analytically, for each pixel of the video frame, a pq-vector corresponding to $\vec{n}_{3D}(i,j) = [p'_{i,j}, q'_{i,j}]^T$ was calculated by using the linear shape-from-shading algorithm. Similarly, for the current pose of the rendered 3D model, corresponding pq-vectors for all rendered pixels were also extracted by differentiating the z-buffer. The similarity of the two images was determined by evaluating the dot product of corresponding pq-vectors:

$$\phi(\vec{n}_{3D}(i,j), \vec{n}_{img}(i,j)) = \frac{|\vec{n}_{3D}(i,j) \cdot \vec{n}_{img}(i,j)|}{|\vec{n}_{3D}(i,j)| \cdot |\vec{n}_{img}(i,j)|} \tag{2}$$

By applying a weighting factor that is proportional to the norm of $\vec{n}_{3D}$, the above equation reduces to

$$\phi_w(\vec{n}_{3D}(i,j), \vec{n}_{img}(i,j)) = \frac{|\vec{n}_{3D}(i,j) \cdot \vec{n}_{img}(i,j)|}{|\vec{n}_{img}(i,j)|} \tag{3}$$

Subsequently, by incorporating the mean angular differences and the associated standard deviations σ, the following similarity function is formed:

$$S = \frac{1}{\sum\sum(\phi_w)\sum\sum(|1-\sigma(\phi_w)| \cdot |\vec{n}_{3D}|)} \tag{4}$$

By minimising the above equation, the optimum pose of the camera for the video image can be derived. The reason for introducing a weighting factor in Equation 4 is due to the fact that pq estimation from the 3D model is more accurate than that of the shape-from-shading algorithm. This is because it is not affected by surface textures or rapid variations of surface reflective properties. The weighting factor therefore reduces the potential impact of erroneous pq-values from the shape-from-shading algorithm and improves the overall robustness of the registration process.

3.2. Simplified Bidirectional Reflectance Distribution Function

Modelling the BRDF of any real world material generally requires the representation of a function over a multi-dimensional domain of at least four parameters, $(\theta_i, \phi_i, \theta_r, \phi_r)$. Fortunately the specific illumination configuration of most bronchoscopes impose restrictions on lighting conditions and allows a number of simplifying assumptions to be made:

- There is only one light source and it always coincides with the viewpoint. That is, $\theta_i = \theta_o$ and $\phi_i = \phi_o$.
- The inner airway surface is assumed to be isotropic. Thus, the BRDF is independent of ϕ_i and hence can be modelled as a function of θ_i only.
- The intensity of light incident on a surface depends mainly on distance from light source and the width of the airway.
- The BRDFs of the different tissues visible in the bronchial lumen can all be modelled as members of a single family of functions, differing only by a scaling factor.
- Surface points with any given BRDF are uniformly distributed.

By taking the above into consideration, the illumination conditions within the airway were modelled by using a lower order polynomial parameterised on the normalised scalar product of viewing vector $\vec{V}$ and surface normal $\vec{N}$ at point, **p**.

$$\rho_p(\vec{V}, \vec{N}) = \sum_0^3 c_i B_i^3(\gamma) \tag{5}$$

where, γ is the cosine of the angle between the viewing direction $\vec{V}$ and the surface normal $\vec{N}$,

$$\gamma = \frac{\vec{V} \cdot \vec{N}}{|\vec{V}||\vec{N}|} \tag{6}$$

and $B_i^n(t)$ are the Berstein polynomials,

$$B_i^n(t) = \frac{n!}{i!(n-i)!}(1-t)^{n-i}t^i \tag{7}$$

This function cannot account for all variations in shade since intensity also depends on distance from light source. This depth dependent effect was also modelled by a low order polynomial:

$$\rho_p(z) = B_0^3(r) + \sum_1^3 d_i B_i^3(r) \tag{8}$$

where $r = (z - z_{min})/(z_{max} - z_{min})$ and z is the distance of the surface point from the viewpoint. The linear shift of the parameter, z, was needed to avoid errors due to extrapolation. The shade of a surface point observed from viewpoint, $\mathbf{p}$, is thus:

$$\Psi_p(\vec{V}, \vec{N}, z) = \rho_p(\vec{V}, \vec{N})\rho_p(z) \tag{9}$$

3.3. Back projection and Parameter Estimation

For each $\mathbf{p}$ there is a unique set of parameters, $(c_0, c_1, c_2, c_3, d_1, d_2, d_3)$, that determines the intensity of every visible point in the 3D model. These parameters were estimated by finding the normal and depth corresponding to each pixel via backprojection and then fitting Ψ to the pixel intensities. Each pixel in the video image was backprojected onto the reconstructed 3D geometry using the position of the bronchoscope that was determined through 2D/3D registration. The following cost function is then minimised over all pixels:

$$C_p = \sum_i (\Psi_p(\vec{V}_i, \vec{N}_i, z_i) - P_i)^2 \cdot w_i \tag{10}$$

where P_i is the pixel intensity. To ensure that Ψ fits the sample points adequately in areas of low sample point density a weighting factor, w_i, was included to compensate for the non-uniform distribution of samples. w_i was set to the inverse of the sample density, estimated via a histogram evaluated over the (γ, z) domain.

3.4. Texture Mapping and Generating New Views

A texture atlas [LPRM02] was generated using the polygonal mesh that was reconstructed from the CT scan of the bronchial tree. The texture was extracted from each video frame by dividing the pixel intensities by $\Psi(\gamma_i, z_i)$, backprojected onto the 3D model and finally, mapped to the texture atlas. Multiple textures were combined into a single map using weighted averaging. Since low intensities often yielded unreliable texture values, weights were initially set proportional to the intensities predicted by the Ψ function, however this yielded very blurry textures. Instead, the maximum weight for each texture element over all texture maps is determined, and texture maps with weights less than maximum are reduce to a very small value. The resulting weight maps were then smoothed in the texture domain prior to merging. This yielded sharper textures while reducing discontinuities. To generate a new view from a view point, $\mathbf{p}_{new}$, the nearest point, $\mathbf{p}$, was found for which Ψ_p had previously been estimated. The 3D geometry was raycast from $\mathbf{p}_{new}$, and the surface normal and depth information were converted to intensities using Ψ_p. This was then multiplied by texture values at corresponding points in the global texture map.

4. Results

The proposed method was implemented in Microsoft Visual C++ on a conventional PC machine (2 GHz Intel Pentium 4 processor, 512MByte main memory, nVidia GeForce 4 MX 440 graphics card, with Microsoft Windows 2000 operating system). Surface rendering was implemented using OpenGL The interface was based on FLTK (http://www.fltk.org).

4.1. In-vivo Validation

The video images were pre-processed to remove the effects of interlacing, lens distortion and unnecessary texture information. These steps are schematically illustrated in Figure 2. De-interlacing is necessary as temporal mismatch of odd-even scanlines can introduce significant errors to the *pq*-space estimation. Barrel distortion caused by the bronchoscope's wide-angle lens was corrected by calculating a distortion centre and correcting for both radial and tangential components. These parameters were determined via the method proposed by Zhang *et al* [Zha00] in which a closed-form solution is used. To remove noise and image artefacts, anisotropic filtering was applied to each image. The method uses a local orientation and an anisotropic measure of level contours to control the shape and extent of the filter kernel and thus ensures that corners and edges are well preserved through out the filtering process.

4.2. 2D/3D Registration

Qualitative results from the in vivo validation are demonstrated in Figure 3, where sample frames from the video sequence are displayed. The proposed *pq*-space based registration has been applied to a video sequence of 31 seconds (797 frames) of the one-patient study. The bronchoscope video sequence starts from the main bifurcation and continues through the left bronchi. Visual inspection of the real and the virtual endoscope images proves that the *pq*-based registration technique can track the tip of the bronchoscope relatively accurately and is stable under sudden movements or

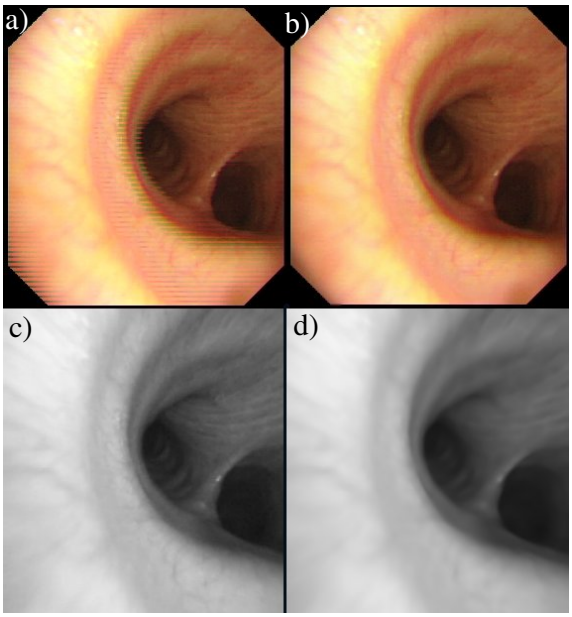

Figure 2: *The pre-processing steps applied to the bronchoscope videos before 2D/3D registration.* ***(a)*** *Original video frame acquired from the prototype bronchoscope,* ***(b)*** *de-interlaced video frame,* ***(c)*** *after lens distortion correction, and* ***(d)*** *final smoothed image by using an anisotropic filter that preserves local geometrical features.*

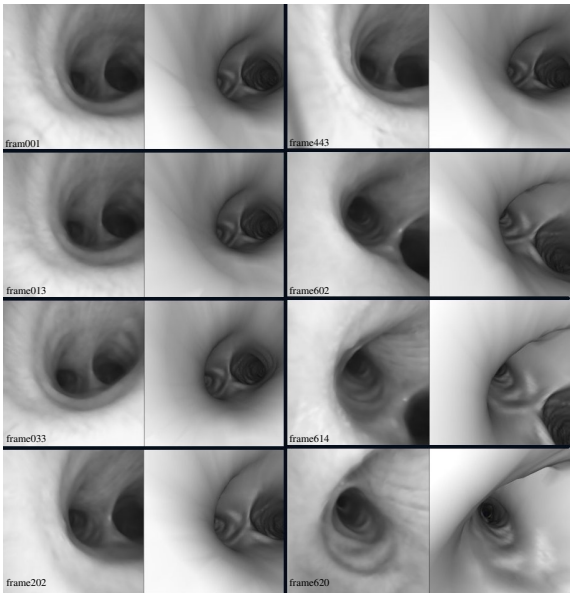

Figure 3: *Example results of in vivo camera tracking for the patient studied in this paper. The left column shows samples of real bronchoscopic images and the right column presents the matched virtual bronchoscopic images after pq-space based 2D/3D registration.*

Absolute error	position (mm)	angle (rad)
Mean	3.50	0.059
Standard deviation	2.42	0.058

Table 1: *Quantitative assessment of pq-space 2D/3D registration*

large rotation angles. However, similar to Mori [KYJ*02], when mis-tracking occurs in one frame, tracking of subsequent frames almost always fails, as the initial starting position deviates too far away from the correct result. Later in the video, bubbles and deformation occlude and distort the anatomical features, and *pq*-based registration fails to work under these conditions.

The video frame sequence was also registered manually and the results used as ground truth in order to estimate the error of the *pq*-space 2D/3D registration method. Table 1 summarises these results and indicates that the method can be accurate to within 4mm positionally.

4.3. IBMR Visualisation

The BRDF and illumination parameters were estimated for 9 frames selected from the set of bronchoscopy video frames to which 2D/3D registration had been applied. Note that the pre-processing applied to these video frames consists of de-interlacing and radial distortion correction only. A texture map was extracted from each of these frames using the estimated BRDF. A global texture map which is independent of shading variations due to BRDF and global illumination, was created by merging all the texture maps together. Finally, this texture map was used to generate new views of the polygonal bronchial tree model. Figure 4 shows the final rendered results using the proposed architecture. It is evident that the rendered results retain the photo-realism required despite the significant changes in viewing position and direction.

5. Conclusion

In summary, we have presented a novel architecture that combines a robust 2D/3D registration technique with BRDF modelling to recover intrinsic surface properties of the bronchial tree. The framework has been tested with real patient data in which each 2D video bronchoscope image is factorised into a surface shading function and texture map so that new views can be rendered with photo-realistic appearance. The restricted lighting configurations imposed by the bronchoscope have been exploited to significantly simplify the BRDF model for predicting the expected shading intensity so that a texture map independent of lighting conditions can be extracted. The current method relies on high accuracy of the initial 2D/3D registration, but in reality this is difficult

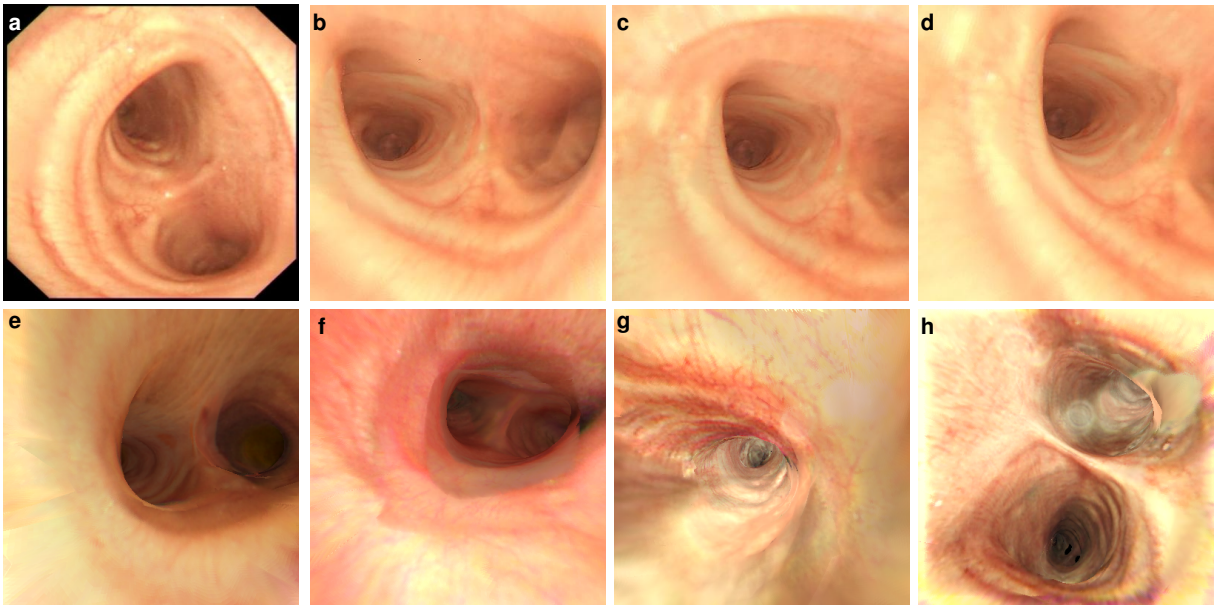

Figure 4: ***(a)****A typical frame captured from the video stream output of the bronchoscopy video processor is shown here.* ***(b-d)*** *New views of the bronchial lumen were generated using texture maps merged from the training video frames.* ***(e-h)*** *Results when applied to different patients. In* ***g-h*** *drops of mucous on the camera lens are treated as part of the surface texture.*

to guarantee particularly in the presence of airway deformation between pre-operative CT and bronchoscope examination. Improving robustness and accuracy of 2D/3D registration in the presence of pre-operative and intra-operative deformation, and the merging of texture maps that tolerate varying degrees of mis-registration error is the topic of future research.

For more information on the VIS-a-VE project see: http://vip.doc.ic.ac.uk/~gzy/vis-a-ve

References

[BG01] BOIVIN S., GAGALOWICZ A.: Image-based rendering of diffuse, specular and glossy surfaces from a single image. In *SIGGRAPH 2001, Computer Graphics Proceedings* (2001), Fiume E., (Ed.), Annual Conference Series, ACM Press / ACM SIGGRAPH, pp. 107–116. 3

[CDS*04] CHUNG A. J., DELIGIANNI F., SHAH P., WELLS A., YANG G.-Z.: Enhancement of visual realism with brdf for patient specific bronchoscopy simulation. In *Medical Image Computing and Computer-Assisted Intervention (MICCAI 2004) 7th International Conference, Saint-Malo, France* (2004), Springer LNCS 3217, pp. 486–493. 1

[CR03] CHUI H., RANGARAJAN A.: A new point matching algorithm for non-rigid registration. *Computer Vision and Image Understanding 89*, 2–3 (2003), 114–141. 2

[CYC*97] CHINN R. J. S., YANG G. Z., CONGLETON J., MELLOR J., GEDDES D. M., HANSELL D. M.: Three-dimensional computed tomography bronchoscopy using clinical datasets: a comparison with fibreoptic bronchoscopy. *Clinical Radiology 52* (1997), 830–836. 2

[DCY03] DELIGIANNI F., CHUNG A., YANG G.-Z.: pq-space 2d/3d registration for endoscope tracking. In *Conference on Medical Image Computing & Computer Assisted Intervention (MICCAI03)* (2003), vol. 1, pp. 311–318. 1, 3

[DvGNK99] DANA K. J., VAN GINNEKEN B., NAYAR S. K., KOENDERINK J. J.: Reflectance and texture of real-world surfaces. In *ACM Transactions on Graphics* (1999), vol. 18 (1), pp. 1–34. 3

[GHW92] GILLIES D. F., HARITSIS A., WILLIAMS C. B.: Computer simulation for teaching endoscopic procedures. *Endoscopy 24* (1992). 2

[HJR*96] HARA A. K., JOHNSON C. D., REED J. E., AHLQUIST D. A., NELSON H., EHMAN R. L., MCCOLLOUGH C. M., ILSTRUP D. M.: Detection of colorectal polyps by computed tomographic colography: feasibility of a novel technique. *Gastroenter 110* (1996), 284–290. 2

[Hor77] HORN B. K. P.: Understanding image intensities. *Artificial Intelligence 8*, 2 (1977), 201–231. 3

[HSH*99] HIGGINS W. E., SHERBONDY A. J., HELFERTY J. P., KIRALY A. P., MCLENNAN G., HOFFMAN E.: Pc-based system for automated quan-

titative virtual bronchoscopy. *Radiology 213* (1999). 1

[HTSG91] HE X. D., TORRANCE K. E., SILLION F. X., GREENBERG D. P.: A comprehensive physical model for light reflection. *Computer Graphics 25*, 4 (July 1991), 175–186. 3

[KYJ*02] K.MORI, Y.SUENAGA, J.TORIWAKI, J.HASEGAWA, K.KATAA, H.TAKABATAKE, H.NATORI: A method for tracking camera motion of real endoscope by using virtual endoscopy system. In *Proc. of SPIE, 3978* (2000-02), pp. 134–145. 2, 6

[LKG*03] LENSCH H. P. A., KAUTZ J., GOESELE M., HEIDRICH W., SEIDEL H.-P.: Image-based reconstruction of spatial appearance and geometric detail. *ACM Transactions on Graphics 22*, 2 (Apr. 2003), 234–257. 3

[LPRM02] LÉVY B., PETITJEAN S., RAY N., MAILLOT J.: Least squares conformal maps for automatic texture atlas generation. In *Proceedings of the 29th Conference on Computer Graphics and Interactive Techniques (SIGGRAPH-02)* (New York, July 21–25 2002), Spencer S., (Ed.), vol. 21, 3 of *ACM Transactions on Graphics*, ACM Press, pp. 362–371. 5

[LW94] LAFORTUNE E. P., WILLEMS Y. D.: *Using the Modified Phong BRDF for Physically Based Rendering*. Technical Report CW197, Department of Computer Science, Katholieke Universiteit Leuven, Leuven, Belgium, Nov. 1994. 3

[MDS*02] MORI K., DEGUCHI D., SUGIYAMA J., SUENAGA Y., AN D C. R. MAURER JR. J. T., TAKABATAKE H., NATORI H.: Tracking of a bronchoscope using epipolar geometry analysis and intensity -based image registration of real and virtual endoscopic images. *Medical Image Analysis 6* (2002), 321–336. 2

[MG97] MOUTSOPOULOS K. N., GILLIES D. F.: Defomable models for laparoscopic surgery simulation. *Journal of Computer Networks and ISDN Systems 29*, 14 (1997), 1675–1683. 2

[PF04] PRADOS E., FAUGERAS O.: *A rigorous and realistic Shape From Shading method and some of its applications*. Tech. Rep. Report nr RR-5133, INRIA, Odyssie Lab, Sophia Antipolis , France, Mar. 2004. 4

[RB92] RASHID H. U., BURGER P.: Differential algorithm for the determination of shape from shading using a point light source. *Image and Vision Computing 10*, 2 (1992), 119–127. 4

[SHH98] STUDHOLME C., HILL D. L. G., HAWKES D. J.: An overlap invariant entropy measure of 3d medical image alignment. *Pattern Recognition 32*, 1 (1998), 71–86. 2

[Vio97] VIOLA P.: Alignment by maximization of mutual information. *International Journal of Computer Vision 24*, 2 (1997), 137–154. 2

[YDMH99] YU Y., DEBEVEC P., MALIK J., HAWKINS T.: Inverse global illumination: Recovering reflectance models of real scenes from photographs. In *Proceedings of the Conference on Computer Graphics (Siggraph99)* (N.Y., Aug.8–13 1999), Rockwood A., (Ed.), ACM Press, pp. 215–224. 3

[Zha00] ZHANG Z.: A flexible new technique for camera calibration. *IEEE Transactions on Pattern Analysis and Machine Intelligence 22*, 11 (2000), 1330–1334. 5